Biophysical Chemistry 20 (1984) 305–317
Elsevier

BPC 00886

LINEAR FREE ENERGY RELATIONSHIP FOR OSMOTIC WATER FLOW THROUGH A MEMBRANE

BENT H. HAVSTEEN

Institute of Biochemistry, University of Kiel, Kiel, F.R.G.

Received 9th November 1983
Revised manuscript received 21st May 1984
Accepted 4th June 1984

Key words: Linear free-energy relationship; Osmotic flow; Membrane transport

A linear free-energy relationship has been found for the osmotic water flux through membranes in a broad variety of systems including electrolytes, organic compounds, intact biological cells and industrial scale filtration. In all cases, broad concentration ranges were found in which the equation $\ln v = \alpha \ln m + \beta$ (v, flux (in kg cm^{-2} min^{-1}; m, molarity)) was valid. The parameters α and β were interpreted in terms of molecular weight, mean ionic radius, enthalpy of solvation, electronic structure and H-bonding propensity. The equation is independent of the membrane material and of the presence of other solutes and precipitates, as long as the latter are incompressible. Its parameters are only slightly dependent upon the temperature. The contributions from different solutes to the osmotic flux are at appreciable concentrations even additive. The relationship permits the prediction of the osmotic water flux and of the rate of filtration of systems of known composition. For simple systems it permits determination of the molecular weight, mean ionic radius, degree of hydration and enthalpy of solvation. It is suggested that osmosis is primarily due to the shift of hydration equilibria and that guanidine hydrochloride, in a realistic concentration range, forms practically infinite clathrates with water. The properties of the urea and Gdn·HCl systems indicate that these solutes either reversibly change the membrane structure and/or display intrinsic hysteresis.

1. Introduction

Linear free-energy relationships were originally discovered by physical organic chemists who subsequently found numerous examples among series of related carbon compounds [1,2]. Eigen [3] has developed a general theoretical explanation of the phenomenon which suggests that it also is valid in other branches of chemistry. This was confirmed for organophosphates by the discovery of solvent dependence of spectral shifts [4]. The property which is examined in this paper, the kinetics of osmotically driven water transport through a membrane, is also related to solvation but the experimental parameter which is varied here is not the polarity of the solvent but the concentration of the slowly permeating solute. Another new finding from the present approach is that some of the solutes, like urea and guanidine hydrochloride, interact with the solvent so as to change the properties of the latter, not only in the vicinity of the solute molecules but probably also propagating into the far range.

The static properties of osmosis have been extensively studied for about a century [5] but the kinetics of the phenomenon seems to have been entirely overlooked [6], at least as far as its concentration dependence is concerned. The approach which has been chosen for this work appears in an experimentally very simple way to offer new insight into the nature of osmosis, the structure of water and the size of hydrates. Besides, the simplicity of the relationship found, as well as its applicability to a wide range of systems and scales including those of chemical engineering and biology, may well provide a suitable basis for the

prediction of the properties of systems which have not previously received attention.

2. Materials and methods

2.1. Materials

The membranes used were asymmetrical and made of cellulose acetate or polycarbonate. The former were donated by DDS (Danish Sugar Manufacturing Co.), Copenhagen. Their permeability for NaCl was 1, 5 and 10% of solute concentration after 5 h at 20°C and 1.5 MPa for M999, M995 and M990, respectively. The polycarbonate membranes were purchased from Nuclepore Corp. They were manufactured with conical pores of a diameter which excludes substances of $M > 50$. The active layer, which was 0.1–0.5 μm, was supported by a 150–300 μm thick highly porous structure.

All reagents were of analytical grade and purchased from Merck, Darmstadt, or Fluka, Neu-Ulm. The water was deionized and, for solutions of high osmolarity, degassed.

2.2. Methods

The kinetic measurements were performed with a double chamber (Lucite) in which the membrane (rectangular, 5 × 5 cm) separated the compartments (volume: 62.5 cm^3 each) (see fig. 1). The chamber which contained the solute was furnished with a vertical glass tube (38 cm long) of 1 mm inner diameter and a magnetic stirring bar. The permeate was allowed to escape through the glass tube and its rubber mouthpiece to a weighing glass where it was collected. The glass was replaced at measured times and weighed. The volume of the permeate which was used to correct the solute concentration for dilution was calculated from the weight and the known density. The flux (v_{20}) was corrected for the effect of temperature on the viscosity of water and expressed in kg permeate at 20°C/m^2 membrane area per min. Since the measurements, with a few exceptions (see below), were made at temperatures near 20°C (20–24°C) and since it could be shown that the kinetically and energetically decisive processes were located in the downflow chamber and not in the membrane, the empirically known viscosity dependence upon temperature was used and the problem of defining viscosity in the membrane was circumvented. The linear flow rate was measured on the ruled escape tube with a stopwatch. In all experiments in which the effect of convection was studied, the rate of revolution of the magnetic stirrer was kept the same. No solute was detectable in the chamber on the upflow side of the membrane. Hence, backflow of solute could be regarded as negligible in the time range of observation. The transport process through the membrane was for both solute and mobile solvent (water) regarded as a chromatographic process. Both solute and water were considered as partitioned between localities of different polarity within the membrane. The driving force for the water transport was assumed primarily to be hydration reactions on the high-pressure side of the membrane and that for the solute was presumably its concentration gradient, i.e., the entropy. The low rate of solute penetration of the membrane, regardless of the molecular size of the solute, may probably be ascribed to the fact that its concentration even inside the membrane is much lower than that of water.

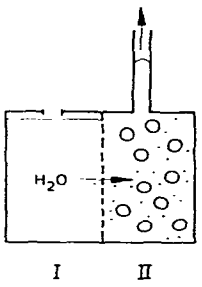

Fig. 1. Sketch of the construction principle of the double chamber for measurement of osmotic flux. Membrane area, 5 × 5 cm; volume of each chamber, 62.5 cm^3; escape tube, 1 mm inner diameter; height of outlet above chamber top, 38 cm.

3. Results

The dependence of the flux of permeate, v_{20}, upon the molarity of NaCl, m, could be linearized

by neither reciprocal nor semilogarithmic plots but yielded in a double-logarithmic plot a line of a very high correlation coefficient ($\ln v = \alpha \ln m + \beta$: see eq. 1 and fig. 2). Therefore, a power function describes the relationship well. The same result was obtained when the flux was replaced by the linear flow rate.

The relation was tested with about 25 substances of widely different nature, singly or in combination. The results are listed in table 1. Most of the non-electrolytes and the simple salts of low molecular weight yielded a single line, whereas urea, guanidinium hydrochloride, LiCl, $AlCl_3$, and most salts of transition metals of the fourth period yielded two lines intersecting in a rather sharp transition point (see fig. 9). Urea and guanidinium hydrochloride even displayed properties resembling hysteresis (see figs. 14 and 15). Near the saturation concentration the curve occasionally dropped due to crystallization. This phage change removed solute from the solution, thus lowering the driving force for the water transport through the membrane (see fig. 9).

In most cases, forced convection from the magnetic stirrer raised the flux by about 10%. This effect was especially marked by solutions of high viscosity, e.g., those containing sugars in high concentration. In the case of sucrose, the rate of revolution of the magnetic bar was increased considerably in a separate experiment which yielded a further small increase in permeate flow rate. Hence, the limit had almost been reached by the standard mixing procedure. Since the double chamber was made of a transparent material, it was often possible to observe the flow pattern of the permeate by colour differences or Schlieren pattern. In the absence of forced convection, the permeate rose to the chamber ceiling on the downflow side of the

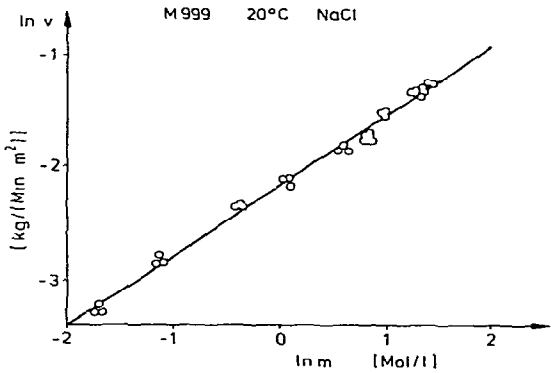

Fig. 2. Flux vs. potential diagram for NaCl at 20 °C. Membrane: cellulose acetate, M999. v, volume flux i (kg permeate/m² membrane area per min); m, molarity; α, slope (= 0.626); ordinate intercept, $I = \beta = -2.164$; correlation coefficient, $r = 0.996$. Line; regression line.

Table 1
Membrane: M999 from DDS. Permeability: 1% for NaCl, 20 °C, 1.5 MPa.

Substance	α [a]	β [a]	r [a]	Concentration [b] (mol/l)
Glucose	0.466	−2.593	0.977	0.30–2.6
Trisodium citrate	0.507	−2.040	0.993	0.05–1.11
Sucrose	0.494	−2.809	0.982	0.07–2.7
Malic acid	–	−2.306	–	1.0 [c]
NaCl	0.626	−2.164	0.996	0.16–4.5
KCl	0.562	−2.962	0.998	0.36–3.3
NH_4Cl	0.647	−1.910	0.997	0.08–2.5
LiCl	0.549	−2.181	0.997	0.14–1.5
	0.711	−2.437	0.981	2.58–7.40
$CaCl_2$	0.528	−1.872	0.994	0.11–5.75
$MgCl_2$	0.572	−1.987	0.967	0.12–3.7
Na_2SO_4	0.520	−1.936	0.997	0.08–1.22
$(NH_4)_2SO_4$	0.527	−1.915	0.994	0.14–2.12
$MnCl_2$	0.707	−1.685	0.996	0.06–0.29
	0.539	−1.882	0.994	0.29–1.0
$FeSO_4$	0.515	−2.536	0.995	0.11–0.12
$CoCl_2$	0.628	−1.827	0.998	0.12–0.78
	0.532	−1.860	0.996	0.78–3.5
$NiCl_2$	0.673	−1.586	0.999	0.05–0.45
	0.519	−1.735	0.996	0.61–3.32
$CuCl_2$	0.576	−1.881	0.995	0.16–1.5
$ZnCl_2$	0.701	−1.520	0.998	0.06–0.33
	0.494	−1.806	0.986	0.37–2.9
$AlCl_3$	0.656	−1.724	0.997	0.11–0.47
	0.448	−1.866	0.985	0.47–1.35
Urea	1.191	−4.480	0.982	5.47–9.97 [d]
	0.615	−3.500	–	2.25–5.47
Guanidine hydrochloride	1.004	−2.900	0.984	1.82–4.95 [e]
	0.553	−2.20	–	1.82–4.95 [f]

[a] Correlation coefficient.
[b] Range of validity.
[c] For the initial experiments with a newly reconditioned membrane valid for concentrations from 2 M.
[d] Valid for initial measurements with membrane conditioned in water.
[e] Valid for membrane conditioned in guanidine hydrochloride.
[f] Parameters pertaining to eq. 1 (see text).

membrane, since its density was less than that of the solution and the diffusion was slow. Forced convection visibly disrupted the concentration gradient between permeate and solution, thus improving the contact between water and solute. Analysis of the collected permeate showed that its solute concentration was about an order of magnitude lower than that in the downflow chamber.

The polycarbonate membrane yielded the same relationship as that found using the cellulose acetate membrane as did biological cell membranes. Therefore, the relation appears to be independent of the material employed However, the irreversibility of the early studies using a cellulose acetate membrane in a strongly hydrogen-bonding solvent such as urea or guanidinium hydrochloride suggests that changes in the microcrystallinic structure of the membrane due to the denaturant take place in the course of time.

3.1. The dependence of the kinetic parameters upon the molecular dimensions

A plot of the slope in the ln v_{20} vs. ln m line as a function of the molecular weight, M, or the molecular diameter (regarding salts as close ion pairs) yielded a vertical asymptote at the parameters of water (see figs. 3 and 4). In an attempt to linearize the relationship, the molecular weight of water was therefore subtracted from that of the substance being tested. When the slope, α, was plotted as a function of $(M-18)^{-1}$ (or the equivalent plot using molecular diameters), a straight line of a high correlation coefficient was obtained for all but a few special cases, e.g., those involving transition metals (see figs. 4, 6 and 8–10). A similar plot for β was only linear for simple 1 : 1 electrolytes (see fig. 5).

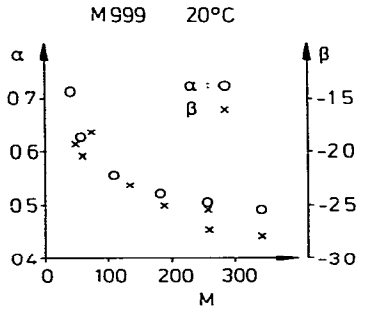

Fig. 3. Dependence of the parameters α and β at 20 °C of some simple substances upon the molecular weight M. Membrane, M999.

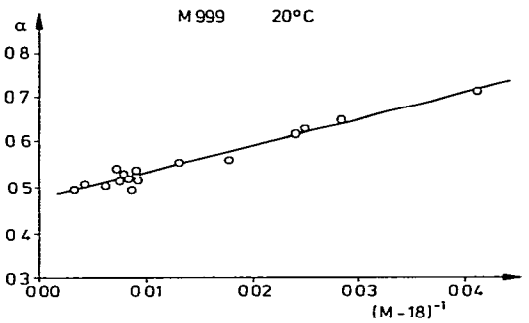

Fig. 4. Dependence of the parameter α (see eq. 1) for further substances upon the function $(M-18)^{-1}$. Slope, 5.705; ordinate intercept, 0.479; correlation coefficient, 0.958.

A test was made of the additivity of the contribution of several different solutes to the osmotic flux. This rule was obeyed for mixtures of sucrose and NaCl, even at high concentrations (see figs. 6 and 7). Hence, these solutes do not significantly

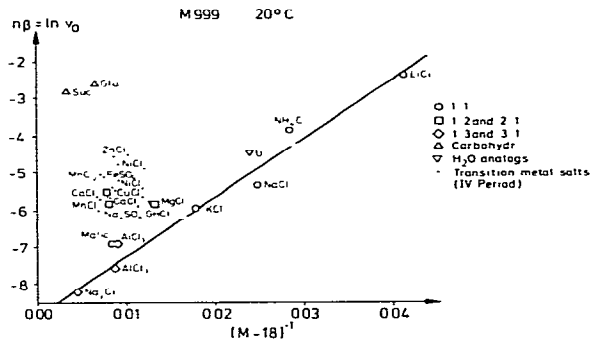

Fig. 5. Dependence of the parameter $n\beta$ upon the function $(M-18)^{-1}$ n, number of particles dissociated from the substance; β, parameter in eqn. 1; $n\beta = \ln v$; v, standard rate of flux ($m = 1$). (○) 1 : 1 electrolytes. (□) 1 : 2 and 2 : 1 electrolytes. (◇) 1 : 3 and 3 : 1 electrolytes, (△) carbohydrates, (▽) water analogs, (●) salts of transition metals (fourth period). U, urea; GHCl, guanidine hydrochloride; Na_3Ci, citrate; Suc, sucrose; Glu, glucose; malic, malic acid. Slope, 158.69; ordinate intercept, −8.784; correlation coefficient, 0.969.

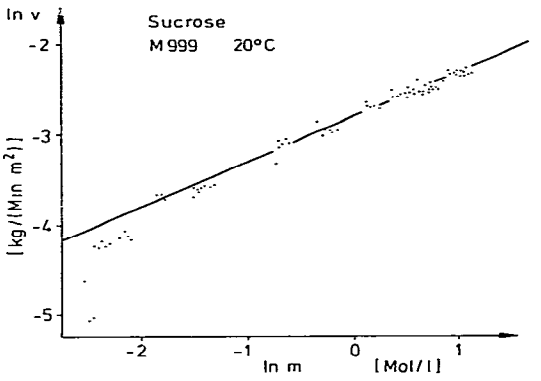

Fig. 6. Flux vs. potential diagram for sucrose at 20 °C. Membrane, M999; $\alpha = 0.494$, $\beta = 2.809$, $r = 0.897$. The drop at very low concentration is probably due to non-conservative forces.

interact under most conditions. The reason is probably the large molar excess of water and the consequence is that predictions may be made of the volume flux of even complex systems.

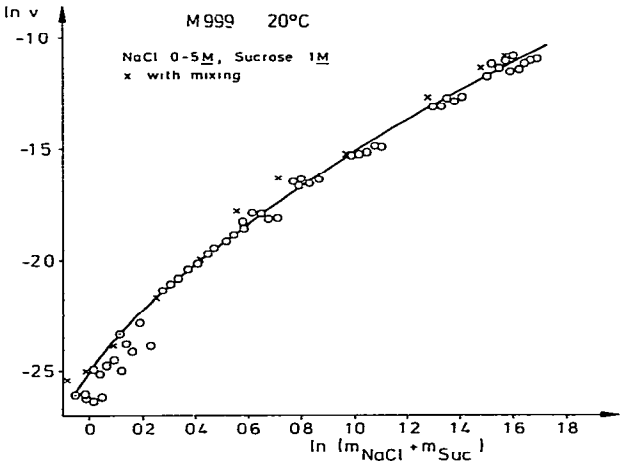

Fig. 7. Flux vs. potential diagram for mixtures of sucrose and NaCl at 20 °C. NaCl, 0–5 M; sucrose, 1 M. (⊙) Without mechanical stirring. (×) stirring with magnetic bar (16 mm long, 8 mm diameter) at 519±35 rpm in solute chamber. Curve, theoretical values; membrane, M999.

3.2. Salts of transition metals from the fourth period

Salts of transition metals were included in the study because of the great propensity of these metals for ligand binding, because their chemically important orbitals (except for $d = 0.5$ and 10) deviate widely from spherical symmetry and because systematic measurements of analogous reactions involving these elements previously have yielded important information [7]. The solubility and cost of suitable salts limited the experiments to the second half of the fourth period.

Since the reach of the d electrons greatly exceeds that of electrons in other orbitals, the kinetic parameters, α and β, were plotted as functions of the number of d electrons which the metal possess. Most of the salts in this group displayed a clear transition point, thus yielding two pairs of kinetic parameters. The low value was used in fig. 11 because the interpretation of data at low solvent concentration is likely to be simpler than that at high values. At high solute concentration, these transition elements hardly show any dependence of the α and β parameters upon the number of d electrons. An exception is Cu^{2+} for which the β value is very low. All data, except those of the copper salt, fall on a smooth curve which can be approximately simulated with an exponential

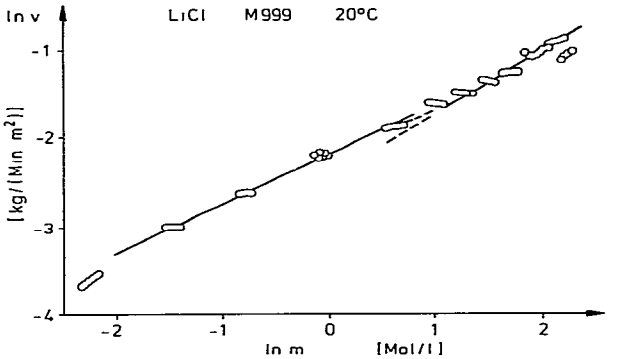

Fig. 8. Flux vs. potential diagram for LiCl at 20 °C. Membrane, M999; $\alpha_1 = 0.711$, $\beta_1 = -2.437$, $r_1 = 0.981$, $\alpha_2 = 0.549$, $\beta_2 = -2.181$, $r_2 = 0.997$. M corresponding to α_2, 103.1 (eq. 2). Line, regression line. The drop at the saturation limit is due to nucleation (visible) and at very low concentration due to non-conservative forces.

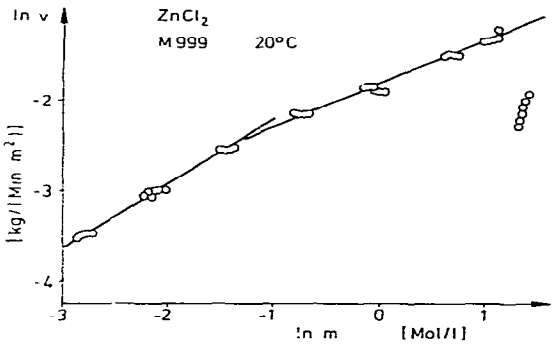

Fig. 9. Flux vs. potential diagram for $ZnCl_2$ at 20 °C. Membrane, M999; $\alpha_1 = 0.494$, $\beta_1 = -1.806$, $r_1 = 0.986$; $\alpha_2 = 0.701$, $\beta_2 = -1.520$, $r = 0.998$. Line, regression line. The drop at the saturation limit is due to crystallization.

curve, but not with a hyperbola or power function (see figs. 11 and 12). Strikingly, the α value for the copper salt coincides with the average of the two sets of parameters which are predicted from the trend in the series (fig. 11). This may be due to the collapse of the bipyramidal complex [10].

When the apparent molecular weight, i.e., that of the hydrate, is calculated from the α parameters, values are obtained which are lower than the formula weight. The relation between α and M is therefore invalid for salts of these transition metals.

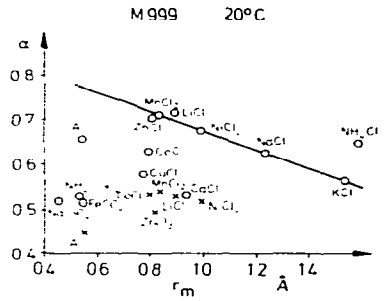

Fig. 10. Dependence of the parameter α upon the mean solute radius [17].

$$\left(\frac{r_-}{2r_-} + \frac{r_+}{2r_+}\right)^{\frac{1}{2}}$$

r_+, number of ions of a given type; r_- radius of ion. (⊙) high or sole value, (×) low value. Membrane, M999; 20 °C. Line, regression line for LiCl, KCl and NaCl.

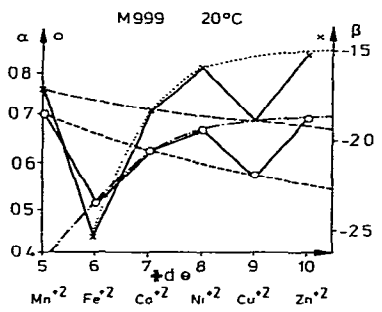

Fig. 11. The dependence of the parameters α and β upon the number of d electrons at 20 °C. Membrane, M999. (⊙) α, (×) β. (– · –) Smooth curve for normal trend in α in the second half period (IV); (· · · · · ·) the same for β, (- - - - - -) trend in α for odd numbers of d electrons;(— — —) the same for β.

The values of the α and β parameters increase with the number of d electrons but apparently not according to any simple law. The reason seems to be the existence of two opposing effects, increase in affinity for water with increasing occupation of the d orbitals (H-bond acceptors) and crowding of electrons in the space near the metal which does not leave room for all of the water molecules which could theoretically be bound in the vicinity of the core of the complex.

3.3. Solutes which form strong hydrogen bonds with water and with their like

Urea showed a single transition point (see fig. 13) but since the line labelled 1 at first was ob-

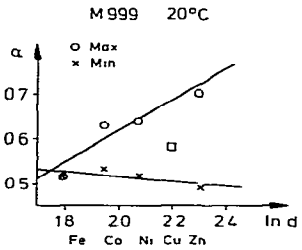

Fig. 12. Fitting of α for salts of divalent transition metals from the second half period (IV) to exponential functions. (⊙) High value, (×) low value, (⊡) Cu. d, number of d electrons. Parameters: maximum: slope = 0.345, $I = -0.0790$, $r = 0.922$; minimum: slope = −0.0513, $I = 0.620$, $r = 0.950$.

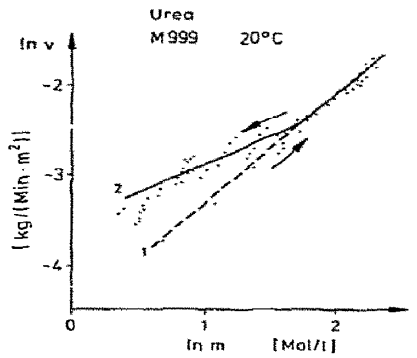

Fig. 13. Flux vs. potential diagram for urea at 20 °C. Membrane, M999. Order of experiments: line 1 from 1 M toward high concentration and back to transition point, then on toward low concentration along line 2 and back to saturation limit; finally back to low concentration along lines 1 and 2. Drop at very low concentration due to non-conservative forces or closure of hysteresis loop. $\alpha_1 = 1.191$, $\beta_1 = -4.480$, $r_1 = 0.982$. $\alpha_2 = 0.615$, $\beta_2 = -3.500$, M_{app} from $\alpha_2 = 60 = M_{urea}$.

tained by increasing concentrations and since its lower part was not retrievable, it appeared that either the solute had caused irreversible changes in the microcrystalline structure of the membrane, or

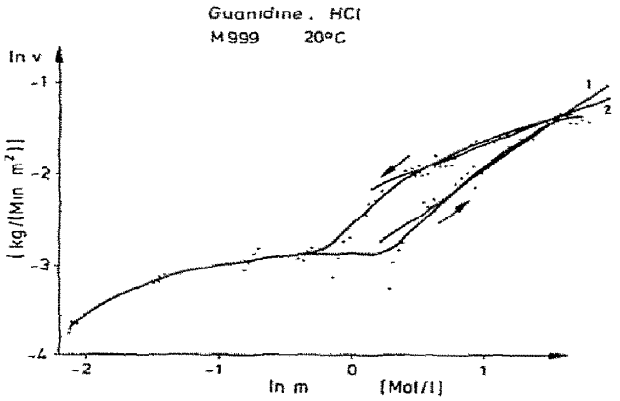

Fig. 14. Flux vs. potential diagram for guanidine hydrochloride at 20 °C. Membrane, M999. Order of experiments: line 1 from 1 M toward saturation limit, back on line 2 to limit of observation; then forward to end of line 1, jump to line 2 and on to saturation limit; finally back on line 2. $\alpha_1 = 1.00 \pm 0.05$, $\beta_1 = 2.900$, $r_1 = 0.984$, $\alpha_2 = 0.55 \pm 0.05$, $\beta_2 = 2.20$, M from $\alpha_2 = 95.5 = M_{Gdn \cdot HCl}$ using eq. 2. Drop at saturation limit due to nucleation.

that the system displayed hysteresis. If the final line, labelled 2 (obtained with decreasing concentrations and confirmed with rising concentrations), was used, the apparent molecular weight obtained from the α-M relation was identical with that of the anhydrous species.

Guanidine hydrochloride exhibited even more complicated properties (see fig. 14). Like urea, Gdn · HCl in the initial experiments yielded the steep line labelled 1. When the concentrations again were lowered, the line labelled 2 was obtained. The latter extends into a curve with steps at still lower concentrations. Finally, the concentrations were increased again, whereby line 2 was obtained anew. The slope of the latter line yielded with the α-M relationship the molecular weight of the unhydrated solute. Since the same membrane was used with both urea and Gdn · HCl, any changes which may occur in the membrane must therefore be reversible.

4. Discussion

4.1. The linear free-energy relationship

The discovery of the power dependence between the water flux, v, through the membrane, and the molarity, m, of the osmotically active solute is in qualitative agreement with the previous observation [8] of an approximate linearity between v and $m^{1/2}$. The latter relationship, which even for many simple substances is rather inaccurate, may be rationalized by considering the dependence of the kinetic energy of solute molecules colliding quasi-inelastically with water-filled membrane pores upon the square of the mass of the impacting particle. In cases where this physical explanation prevails over entropic and chemical contributions to the osmotic water flux, a square root dependence would be expected. However, the impact is probably not elastic, other mechanisms of deactivation of the solute molecules could be envisaged, and the specificity of the kinetic parameters requires the application of a chemical model. The individuality is pronounced, even for simple substances which predominantly have spherical orbitals, like NaCl and $CaCl_2$, but for such salts it

is simply related to the density because the data for these two substances fall on the same straight line when ln v is plotted against the logarithm of the weight percentage of solute.

The power dependence between water flux, v, and molarity, m, may be identified with a linear free-energy dependence in the sense of Brønsted and Hammett because ln v is a linear function of the energy of activation and ln m is linearly dependent upon the chemical potential, μ, of the solute. The latter is in turn linearly dependent upon the affinity of the solute for water. Since both the collision theory (Newton's third law) and the entropic driving force are non-specific phenomena, whereas the effect here observed shows a marked specificity, the interaction between solute and water must be prevailing. Like all 'linear' free-energy relationships, the one discused here is not truly linear but represents in a wide concentration range a very good approximation to linearity.

Onsager [9] postulated a general linearity between any force and its associated flow for systems near equilibrium. Since the present system displays a linearity between the logarithm of the absolute flow, i.e., a measure of the relative flow, and a force created by the chemical affinity of the solute for the water, the general theorem also applies to this system within a certain range of boundary conditions. This requirement is common to all linear free-energy relationships. The explanation is given by Eigen [3]. This is rather surprising, since the conditions here are far from those of thermodynamic equilibrium but the phenomenon may be explained by the narrowness of the range of water concentrations employed. Unfortunately, the water concentrations could not be lowered by the addition of less polar solvents since the latter destroyed the membrane. At low solute concentration, the prediction by Onsager could be verified.

The transitions between different ranges of linearity should probably be interpreted as cooperative changes in hydrate structure, since they are most often exhibited by substances possessing centers of high surface charge density, e.g., Li^+, Al^{3+} and transition metals (see figs. 8 and 9). The strongly hydrogen-bonding solutes, e.g., urea and Gdn · HCl, seem to present a different case. Here, the solute is capable of entering into complexes with water which strongly resemble the solvent's own semicrystalline structures. The concentrations range where the ln v vs. ln m plot of Gdn · HCl yields an asymptotic approach to a horizontal slope appears to represent such a case because this slope corresponds to infinite hydration (high molecular weight).

4.2. The dependence of the kinetic parameters upon the molecular dimensions

In the most simple cases, the data yielded a single straight line in a double-logarithmic plot of flux vs. molarity (see figs. 2 and 6):

$$\ln v = \alpha \ln m + \beta \qquad (1)$$

In an attempt to give the empirical parameters α and β a physical meaning, their correlations to various molecular parameters were tested. These included the molecular weight (M), molecular diameter and enthalpy of solvation. The parameter α corresponds to the Hammett ρ value and to the Brønsted α (or β) value, i.e., it represents the sensitivity of the reaction to a change in driving force. Similarly, the parameter β, the flux at standard concentration of solute (1 M), by Hammett and Bronsted corresponds to the rate of the standard reaction. A simple plot of α vs. M yields a curve with a vertical asymptote at the molecular weight of water. This probably simply means that small molecules can be accommodated more easily in the water structure than large ones. The dependence of v upon r^{-1} (r, radius of the molecule) rather than on r^{-2} may mean that the surface/volume ratio, i.e., the surface charge density, and dipole-dipole interactions, are important factors. This curve (figs. 3 and 4) fits a hyperbola very well for the majority of substances tested. When for electrolytes M was replaced by the sum of the ionic diameters, a fit of similar quality was obtained. In cases (excepting salts of transition metals) where different kinetic parameters were found in different concentration ranges, one of the α parameters (the lower) yielded the properties of the anhydrous species. For LiCl the other α parameter yielded a molecular weight which corresponded to that of the known hydrated species (fig. 8), but for $AlCl_3$ and the salts of the transi-

tion metals, the relationship for unknown reasons became invalid since the apparent molecular weights were smaller than the formula weights. One advantage of the double-logarithmic plot is that activity coefficients only enter into the β parameter. Therefore, the α value may be regarded as thermodynamic which greatly facilitates any interpretation.

There is a close correlation between the enthalpy of hydration of simple 1 : 1 electrolytes and the α parameter (see fig. 15) [23]. The larger the enthalpic contribution to the free energy of solution was, the larger was also the α parameter, i.e., the sensitivity of the flux to changes in the solute concentration. This may be another expression of the above-mentioned phenomenon that solute molecules of approximately the same size as water can lodge themselves in the water structure without much disturbance, more easily than larger ones.

The β parameter which represents the logarithm of the flux at standard solute concentration shows properties similar to those of the α value. However, its correlation with the molecular properties discussed are less precise (see figs. 3 and 5). This indicates that the term β is more complex than that of the α parameter. This must be expected since β not only contains the activity coefficients, which are rather specific for the solute molecules, but also the particle number, i.e., the degree of dissociation of the solute. At this stage, no further attempt was made to analyze β.

The possible interrelation between the parameter α and the mean radius of the electrolyte, defined as $r_m = (2r_+^{-1} + 2r_-^{-1})^{-1}$, has been investi-

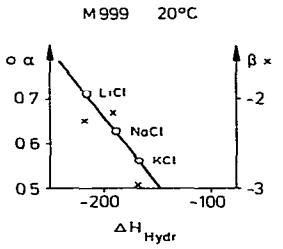

Fig. 15. Dependence of the parameters α and β upon the enthalpy of hydration at 25 °C [21,23]. Line, regression line for α. (⊙) α, (×) β. Slope, −0.00310; ordinate intercept, 0.04198; $r = -0.9999$.

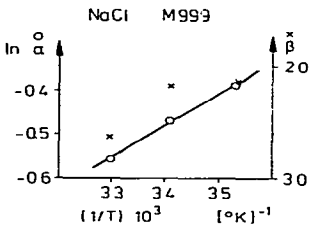

Fig. 16. Temperature dependence of the parameters α and β (eq. 1) upon temperature. (⊙) α, (×) β. Membrane, M999.

gated (see fig. 10) [17]. For a series of analogous simple salts, like the chlorides of Li, K and Na, a strict linear correlation ($r = 0.9999$) was found. Furthermore, it is notable that several other salts yield data which fall on this line. When two α values are found, the second tends to fall in a narrow range between 0.50 and 0.55. Exceptions to the linear correlation are NH_4Cl and $AlCl_3$, which both have a high surface charge density on the metal ion or its equivalent, and the transition metal salts, $CuCl_2$ and $CoCl_2$, which both have peculiar molecular orbitals [10].

4.2. Salts of transition metals of the fourth period

The properties of salts of transition metals were examined in more detail because their representatives with the metals in the oxidation state +2 yielded a poor fit to the relationship between α and $(M - 18)^{-1}$, which is satisfied by most other substances. Furthermore, they are readily available, adequately soluble, and known as avid ligand binders. Since these metals are the lightest and simplest of the elements possessing $3d$ electrons, i.e., orbitals which generally protrude from the spherical centre of the ion (except for $d = 0$, 5, and 10) [16], these salts could be expected to present unique interphases for water binding. At first, the possibility that the number of d electrons was the determining factor was examined (see fig. 12). For both parameters α and β, a smooth curve was found at low solute concentration, when the data for $MnCl_2$ and $CuCl_2$ were excluded. It appears likely that the departure of $CuCl_2$ from the trend in the group is due to the Jahn-Teller-effect, a quantum-mechanical degeneracy, which causes a

distortion of the ligand field and hence the collapse of a bipyramidal structure to that of a square-planar field [10]. In the case of $MnCl_2$, a likely reason for the deviation is that Mn belongs to the first half period. A break in the properties between the half period is known from the kinetic properties [7], ionization potentials [14], energies of electronic pairing [12], hydration energies [13] and ligand field stabilization energies [15]. The curves may be approximated rather well with a single-exponential function through the point of every other element but not with a hyperbola, power function or trigonometric expression. Qualitatively, it appears reasonable to find such a dependence because an increasing number of *d* electrons progressively excludes space for water binding near the core due to electrostatic repulsion. Since the *d* orbitals are normally filled pairwise due to the Pauli exclusion principle, the addition of each new *d* electron might be expected to cause a break in the curve [11]. Therefore, an attempt was made to find a simple relationship when only elements possessing an even number of *d* electrons were considered. Similarly, the parameters of elements with an odd number of *d* electrons were compared. In both cases, a smooth curve which could be fitted with a single-exponential function appeared (stippled curves in fig. 12). This relationship is expected if the probability of an encounter between water and an electron is the prevailing factor. At high solute concentration, water does not seem to interact with the 3*d* electrons (see table 1). The low β value for Cu^{2+} at high solute concentration indicates that only a very limited interaction with water occurs.

4.4. Solutes forming many strong hydrogen bonds with water

Solutes which form many and strong hydrogen bonds resemble water in an important respect and could therefore be expected to show particular osmotic properties. Two typical examples, urea and guanidine hydrochloride, have been chosen for closer examination. Due to their competition with water, both are strong denaturants for proteins and similar polymers.

The ln *r* vs. ln *m* plot for urea shows two linear sections with a sharp transition point. At this point, a change in the hydration structure apparently takes place. In initial experiments, i.e., with an unconditioned membrane, the steeper line (labelled 1) is obtained. The explanation may be that the microcrystalline structure of the membrane, which is also stabilized by hydrogen bonding, is destroyed by the solute. If so, then the process is reversible because after washing, the parameters of simple salts could be confirmed with the same membrane. An alternative explanation is that the system shows hysteresis, a property it should possess, since it is controlled by more than two internal parameters [22]. The remainder of the hysteresis loop may well lie outside the concentration range which permits observation, since the trend of the data on the less steep line (marked 2) to drop below the values expected at very low concentration should probably be ascribed to the prevalence in this range of non-conservative forces, e.g., solvent-membrane- and solvent-solvent-friction. Thus, the latter forces obscure the lower part of the hysteresis loop.

With guanidine hydrochloride, a complete hysteresis loop is obtained (fig. 14). It was determined as indicated on the figure: At first, line 1 was obtained with increasing concentrations. When the concentration was lowered again (in separate experiments, only the membrane was retained), line 2 was obtained. Finally, the concentrations were again increased and lowered anew but all data recorded remained (as with urea) on the upper curve. Gdn · HCl gives rise to a horizontal tangent in the intermediate concentration range. This corresponds to an infinitely high molecular weight which probably means that Gdn · HCl and H_2O form extensive, mixed clathrates. It is striking that the ratio between the slopes of lines 1 and 2 for both urea and Gdn · HCl within experimental error is equal to 2 (1.94 ± 0.18 for urea and 1.82 ± 0.18 for Gdn · HCl). This is also true of the standard flux ratio ($e^{\beta_2}/e^{\beta_1} = 2.01 \pm 0.11$) for Gdn · HCl but not for urea (2.66 ± 0.10). Although the probability that this is a coincidence is low, no simple explanation of the phenomenon is apparent. For both urea and Gdn · HCl, the lower of the α values (α_2) corresponds to the anhydrous molecular weight but α_1 does not correspond to

the molecular weight of the dimer. Whereas the plot for urea results in straight lines, that for Gdn · HCl displays distinct steps. I am inclined to interpret this finding as the prevalence in urea solutions of only two major hydration structures, whereas Gdn · HCl at low concentrations forms a large number, perhaps a continuum, of different hydrate structures but at high concentrations only two. A further restriction is that these two kinds of structure apparently do not coexist.

4.5. Biological examples

The general validity of the relationship found (eq. 1) seemed to be indicated by its applicability to a wide variety of simple systems but the generalization had to be tested on realistic examples, e.g., those found in nature and industry. Firstly, the pre-steady-state phase of the penetration by protons of the mitochondrial membrane after opening of the specific H^+ channel (Cl^- cotransport) was compared with the corresponding phase of the water transport through an artificial membrane [24]. In both cases, the time course was exponential (fig. 17), which could be expected from the relaxation equation.

Secondly, the kinetics of the uptake of water into cytoplasmic vesicles of the sweet water ciliate *Paramecium* was examined at various environmental concentrations of NaCl [25]. A plot according to eq. 1 of the water flux as a function of the NaCl concentration yielded a straight line (see fig. 18). The sign of the slope is negative here which may

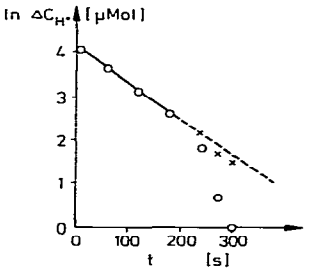

Fig. 17. Rate of proton efflux from mitochondria following the injection of a pulse of 10 nmol O_2. Relaxation times (s): $\tau_1 = 122$, $r = 0.9999$; $\tau_2 = 46$. (⊙) Observed values, (×) data after subtraction of the contribution from the second process.

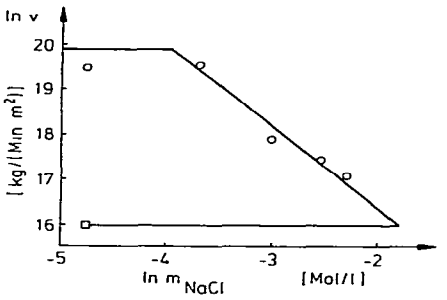

Fig. 18. Active water uptake into cytoplasmic vesicles of the sweetwater ciliate *Paramecium* at 23°C. (⊙) Observed rate of swelling, (⊡) rate after addition of KCN. $\alpha = -1.789$, $\beta = 12.807$, $r = 0.985$.

imply the occurrence of a counter-flow of NaCl through the membrane. Evaluation of the mass of the driving agent according to eq. 2 using the parameters of the synthetic membrane gave a value of 22.4 which is indistinguishable from the atomic mass of Na. If this result is not fortuitous, then the membranes through which the osmotic flow occurs happen to have permeability characteristics similar to those of the cellulose acetate membrane M999. Since inhibition of the active transport processes with KCN eliminated the water flow, an Na^+-activated ATPase appears to be involved. It may maintain electroneutrality at the membrane by exchanging Na^+ for K^+ but could be electrogenic.

Since the results with *Paramecium* indicated that eq. 1 was also applicable to single ions, a similar system involving a different ion was analyzed: the influx of K^+ across the plasma membrane of the duck erythrocyte [26]. In this case, the K^+ flux was measured as a function of the molarity of this ion and plotted according to eq. 1. The dependence is linear (see fig. 19) but evaluation of the mass of the driving agent is not possible, since the parameters required for the use of eq. 2 are not available.

The fourth example of data amenable to testing of eq. 1 is found in studies of the vectorial transport of Ca^{2+} by the plasma membrane ATPase of the human erythrocyte [28]. This enzyme is gated by Ca^{2+}, Mg^{2+} and ATP to assume one of the alternate conformations A or B, each of which has individual enzymatic and translocating capabili-

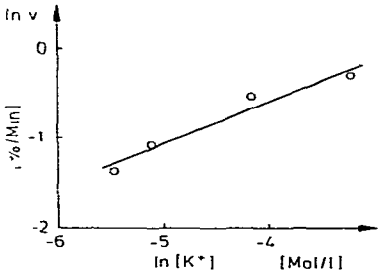

Fig. 19 Rate of K^+ influx into duck erythrocytes. $\alpha = 0.474$, $\beta = 1.299$, $r = 0.974$.

ties. A plot according to eq. 1 yields straight lines within certain ranges of environmental conditions (see Fig. 20). Further evaluation is, in the absence of detailed molecular information, not possible.

4.6. *The nature of osmosis*

Over the years, three different theories have been proposed to explain this ubiquitous and vital phenomenon. One is based on Newton's third law, another on the entropic effect of solute exclusion from one of the compartments and the third rests on the affinity between solute and solvent. All three principles must be valid, so the only remaining question is the relative importance of their contributions to the observed total effect. It is feasible to evaluate and compare the driving forces from each of the three mechanisms but the prevalence of the third already becomes clear when the solute specificity of kinetic parameters α and β is considered. Only chemical reactions can show this property. Therefore, water passes through the membrane to form hydrates of higher coordination number in an equilibrium reaction. The energy of activation of osmotic flux is very low (0.22 kcal/mol for NaCl solutions (see fig. 16)), since the hydration reactions in the systems chosen are very fast. This value is indistinguishable from that of diffusion, about 1 kcal/mol [18,19]. In most systems, especially in those of high viscosity, e.g., those containing sugars, forced convention increases the osmotic flux by 5–10%, depending on the concentration. This finding is in agreement with the hydration hypothesis because convection improves the contact between solute and solvent but conflicts with the entropic and collision mechanisms because the latter would require that the elimination of local concentration gradients lowers the osmotic flux. Osmosis is therefore first of all driven by hydration reactions and the result is the suction of water through the membrane to the solute. The membrane itself apparently only plays a passive role, that of a filter, since solute within the period of observation did not have time to cross the membrane in the opposite direction to that of the water flux. This conclusion is supported by the finding that both membranes, despite their widely different structures, yielded the same osmotic parameters and that convection on the downflow side of the membrane enhanced the water flux.

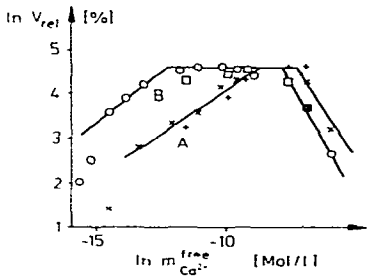

Fig. 20. Rate of Ca^{2+} efflux from ghosts of human erythrocytes and inverted (inside-out) membrane vesicles at 37 °C. Erythrocyte ghosts: (×) ATPase, form A; (⊙) ATPase form B. Inside-out vesicles: (+) Ca^{2+} pump, form A; (⊡) Ca^{2+} pump, form B.

The generality of the relationship between osmotic flux and solute concentration is emphasized by the observation that it is also satisfied by single-cell systems, such as sweet water ciliates [25] and a broad variety of technical filtration systems, with and without filter cake [27]. However, the latter statement must, at least for the present, be restricted to cases in which there is no appreciable formation of compressible filter cake, because I have not yet had the opportunity to test systems with large amounts of such precipitate. Experiments of this nature are in progress but since in such systems the highly non-Newtonean rheology dominates, i.e., non-conservative forces, the prospects of the discovery of a simple flux-force

relationship are not very good. In spite of this, knowledge of the limits of applicability of the rule is valuable. Furthermore, the relationship has been proved to permit better prediction of flow rates than the classical filtration law, which is based on Poiseulles' law [20].

Acknowledgements

Thanks are due to Mrs. R. Thun for technical assistance and to D.D.S. Ltd., Copenhagen, for the gift of cellulose acetate membranes.

References

1 J.N. Brønsted and K. Pedersen, Z. Phys. Chem. 108 (1923) 185.
2 L.P. Hammett, Chem. Rev. 17 (1935) 125.
3 M. Eigen, Angew. Chem. Int. Ed. 3 (1964) 1.
4 M.J. Kamlet, P.W. Carr, R.W. Taft and M.H. Abraham, J. Am. Chem. Soc. 103 (1981) 6062.
5 J.C.W. Frazer, The laws of dilute solutions, 2nd edn. (Van Nostrand, New York, 1931).
6 M.H. Jacobs, Ergeb. Biol. 12 (1935) 1.
7 P. Geier, Habilitation Thesis, University of Zürich (1968).
8 E. Justi and A.W. Winzel, Kalte verbrennung – fuel cells (F. Steiner, Wiesbaden, 1962) p. 77.
9 L. Onsager, Phys. Rev. 37 (1931) 405.
10 H.A. Jahn and E. Teller, Proc. Roy. Soc. A161 (1937) 220.
11 W. Pauli, Z. f. Phys. 31 (1925) 765.
12 L.E. Orgel, J. Chem. Phys. 23 (1955) 1819.
13 P. George and D.S. McClure, Prog. Inorg. Chem. 1 (1959) 381.
14 C.E. Moore, Ionization potentials and ionization limits derived from the analysis of optical spectra, NSRDS-NBS34 (National Bureau of Standards, Washington, DC, 1970).
15 K.F. Purcell and J.C. Kotz, Inorganic chemistry (W.B. Saunders, Philadelphia, 1977, p. 553.
16 K.F. Purcell and J.C. Kotz, Inorganic chemistry (W.B. Saunders, Philadelphia, 1977) p. 552.
17 C.D. Hodgman, R.C. Weast and C.W. Wallace, Handbook of chemistry and physics, 35th edn. (Chemical Rubber, Cleveland, 1953) p. 3089.
18 M. Eigen and L. DeMaeyer, in: Technique of organic chemistry, Vol. 8, part 2, ed. A. Weissberger (Interscience, New York, 1963 p. 1033.
19 M. Eigen and L. DeMaeyer, Z. Electrochem. 60 (1956) 1037; 61 (1957) 856.
20 R.A. Weiler, Proc. Int. Symp. Liquid-Solid Filtration, Antwerp, (Inst. Chem. Eng. UCL, Louvain-la-Neuve, 1978).
21 L. Benjamin and V. Gold, Trans. Faraday Soc. 50 (1954) 797.
22 G. Nicolis and I. Prigogine, Proc. Natl. Acad. Sci. US.A. 78 (1981) 659.
23 D.F.C. Morris, Struct. Bond. 6 (1969) 157.
24 P.C. Hinckle and R.E. McCarty, Sci. Am. 238 (1978) 104.
25 S. Clark, A practical course in experimental zoology, (Wiley, London, 1966) p. 25.
26 F.M. Kregenow, J. Gen. Physiol. 58 (1971) 396.
27 B. Havsteen, J. Chem. Eng. (1984) in the press.
28 O. Scharff, Doctoral dissertation, University of Copenhagen (Fadl, Copenhagen, 1980).